

Orientational Ordering of a Poly(oxyethylene)–Poly(oxybutylene) Diblock Copolymer Gel under Steady Shear Flow

John A. Pople and Ian W. Hamley*

School of Chemistry, University of Leeds, Leeds LS2 9JT, U.K.

J. Patrick A. Fairclough and Anthony J. Ryan†

Department of Chemistry, University of Sheffield, Sheffield S3 7HF, U.K.

Colin Booth

Department of Chemistry, University of Manchester, Manchester M13 9PL, U.K.

Received November 10, 1997; Revised Manuscript Received January 21, 1998

ABSTRACT: Orientational ordering was investigated in the hexagonally packed rod phase formed by a poly(oxyethylene)–poly(oxybutylene) diblock copolymer in concentrated aqueous solution. The resulting soft gel was subjected to steady shear in a Couette cell, with simultaneous small-angle X-ray scattering (SAXS) experiments. Orientation function coefficients were extracted from SAXS patterns to quantify the degree of orientation. It is found that the averaged Legendre polynomial orientational order parameters increase logarithmically with a linear increase in shear rate. A limiting degree of orientation of $P_2 \sim 0.6$ is reached for a shear rate of $\dot{\gamma} = 100 \text{ s}^{-1}$, above which an increase in shear rate does not significantly improve the orientation. Time-resolved measurements reveal that the steady-state degree of orientation was developed within the gel over a time scale $t \sim 30 \text{ s}$ and upon cessation of shear relaxed to an intermediate orientation level over a time scale of $t \sim 1 \text{ h}$.

Introduction

The study of block copolymer microstructure is of increasing interest due to extensive commercial applications. Block copolymers in solution have been shown to self-organize into micellar systems,^{1,2} and these systems have been shown to exhibit a variety of phases, dependent on copolymer concentration and temperature.^{1–3} The material studied here is a diblock copolymer of poly(oxyethylene) (E) and poly(oxybutylene) (B) $E_{18}B_{10}$, (where the subscripts denote the number of repeats), which has been shown to form a hexagonal phase and lamellar and cubic liquid crystal phases in aqueous solution (this material was previously identified as $E_{17}B_{10}$).⁴

In general, shear leads to an enhancement of macroscopic order of the microdomains in block copolymer melts or solutions.^{5–9} There have been only a few studies on the effect of shear on block copolymer solutions. Balsara and co-workers⁵ studied solutions of a poly(styrene)–poly(isoprene) (PS–PI) diblock in the nearly neutral solvent dioctyl phthalate. It was found that for the hexagonal phase of cylindrical micelles (PS core, PI fringe) in concentrated solution, increasing shear rate led to an increase in ordering up to a shear rate $\dot{\gamma} \sim 0.1 \text{ s}^{-1}$ but remarkably led to shear-induced disordering at higher shear rates.⁵ These results are in conflict with theory,⁶ which is only able to predict shear-induced ordering. There has been more work on the effect of shear on the hexagonal phase in block copolymer melts, dating back to the work of Keller and co-workers⁷ who showed using SAXS and transmission electron microscopy (TEM) that PS–PI–PS triblocks can be oriented to a high degree by extrusion. Subse-

quently, Hadziioannou et al.⁸ demonstrated using SAXS that “monodomain” specimens of a hexagonal phase can be oriented by reciprocating shear. This method has recently been widely used by the Minnesota group,^{9–11} Morrison et al.,¹² Winter and co-workers,¹³ and others to study the effect of shear on the hexagonal phase in diblock and triblock melts, and the extensive literature has recently been reviewed.²

Since the block copolymers we study are of low molecular weight, they show phase behavior similar to that of low molecular weight amphiphiles. Thus, comparison can be made with previous studies of the effect of shear on hexagonal phases in conventional surfactants. Richter¹⁴ has presented results from small-angle light scattering (SALS) experiments on nonionic surfactant solutions sheared in a cone-and-plate device and SANS experiments on the same solutions sheared in a Couette cell. An enhancement of SALS intensity along the flow direction indicated that mesoscopically the sample is characterized by an undulation of the director, which is defined as the average orientation of the constituent rodlike micelles. SANS provided evidence that the rodlike micelles were aligned along the flow direction.¹⁴ Viscosity measurements in a cone-and-plate rheometer have been combined with deuterium NMR experiments to investigate the effect of shear on the alignment of the hexagonal phase in the nonionic surfactant hexakis(ethylene glycol) dodecyl ether, $C_{12}E_6$ (C = poly(methylene) in our notation).¹⁵ It was shown that the reorientation of the directors depends only on the shear strain and not the shear rate. We will show in this paper that the orientation of the hexagonal phase in an amphiphilic block copolymer solution is a function of shear rate.

The purpose of the present study was to investigate the effect of steady shear on a diblock copolymer forming

* To whom correspondence should be addressed.

† CLRC Daresbury Laboratory, Warrington WA4 4AD, U.K.

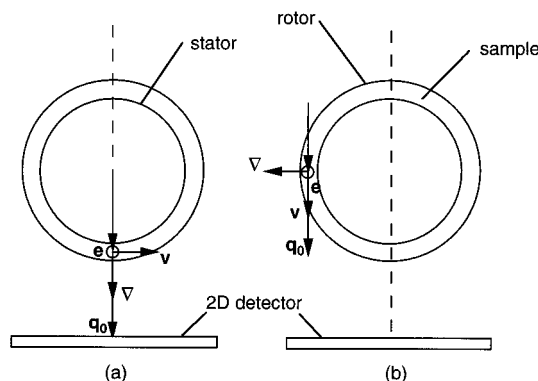


Figure 1. Top view of the Couette cell showing the two geometries for the SAXS experiments. Here \mathbf{v} is the velocity (shear) direction, ∇ is the shear gradient direction and $\mathbf{e} = \mathbf{v} \times \nabla$ is the neutral (vorticity) direction. The incident wavevector is denoted \mathbf{q}_0 . Key: (a) radial projection; (b) tangential projection.

a hexagonal phase in concentrated aqueous solution, and to quantitatively record the resulting orientation. The steady shear was applied in a Couette cell, which enables the shear-induced orientation to be studied in two orthogonal directions, the “radial” and “tangential” aspects, as defined below. The employment of high flux synchrotron sources also permitted time-resolved studies of the development of the shear-induced orientation and observation of the relaxation of the orientation when the shearing was stopped.

Experimental Section

Materials. The material utilized in this work was a diblock copolymer of poly(oxyethylene) and poly(oxybutylene), $E_{18}B_{10}$. The block copolymer was synthesized at the laboratories of the Dow Chemical Co. in a manner previously described,¹⁶ and was used as received. Its composition has been variously described within the range $E_{18}B_9$ to $E_{20}B_{10}$, possibly depending on batch, but more likely because of experimental uncertainty in its characterization. Its micellization behavior and the properties of its micellar solutions, as revealed by surface tension and dynamic light scattering, have been reported.^{17,18} Solutions were prepared by mixing 35 wt % of copolymer in 0.2 mol dm⁻³ aqueous K_2SO_4 at $T = 40$ – 50 °C, followed by several days storage in a refrigerator. This solution formed a birefringent soft gel, consistent with a hexagonal structure. This structure was confirmed by SAXS.

Couette Cell. Time-resolved SAXS data were acquired during steady shear of the gel in a couette cell constructed from aluminum, which has been described previously.¹⁹ Samples were studied under the application of continuous shear at shear rates between $\dot{\gamma} = 0.1$ s⁻¹ and $\dot{\gamma} = 500$ s⁻¹. The geometry of the Couette cell is such that either the “radial” or the “tangential” aspects of the flow field were able to be probed. For the purposes of this work, the “radial” aspect is defined as the X-ray beam travelling normal to the plane containing the shear flow vector and the vorticity vector, which is realized experimentally as the case where the X-ray beam passes through the center of the couette cell (Figure 1a). Similarly the “tangential” aspect is defined as the X-ray probe travelling normal to the plane containing the shear flow gradient vector and the vorticity vector, which is experimentally realized as the case where the X-ray beam passes between the stator and rotor at the edge of the cell (Figure 1b). In the SAXS experiments the flow direction was horizontal.

Small Angle X-ray Scattering. SAXS experiments were performed on the high brilliance beamline ID2 at the ESRF synchrotron facility at Grenoble, France.²⁰ The X-ray beam, of wavelength $\lambda = 0.764$ Å, had a cross section of 0.2 mm diameter at the sample, and a two-dimensional gas filled

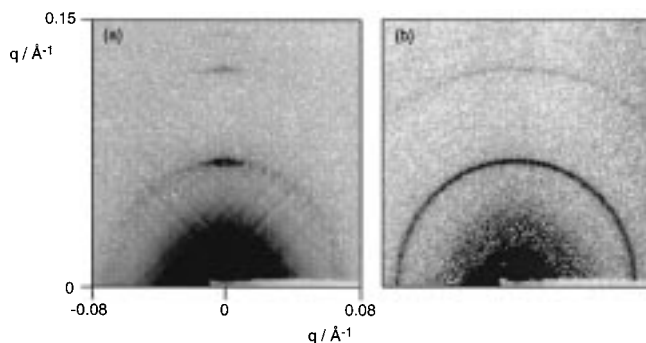


Figure 2. SAXS patterns from the solution subjected to shear at $\dot{\gamma} = 100$ s⁻¹ in the (a) radial and (b) tangential projections. The shear direction was horizontal.

detector with 512×512 pixels was employed to collect the scattered X-rays with a sample-to-detector distance of 5 m.

Determination of Orientational Order Parameters

SAXS reveals information about the gel structure on a scale of ~ 100 Å, which is the approximate length scale of the hexagonal “rod” structure. The anisotropy of the diffraction peaks in the SAXS patterns is related to the orientational ordering of the domains of rods. X-ray scattering proves particularly useful for determining orientational order because a complete characterization of the orientation distribution function is possible: in contrast only the first nonzero orientational order parameter is obtainable from, for example, birefringence measurements. The area of the sample exposed by the incident beam is large in relation to the scattering units, (1 mm cf. 100 Å), and therefore the SAXS patterns provide orientational order parameters that are global averages over the orientation of domains of rods. Within each domain, the average orientation of the rods is described by the director.

To describe the anisotropy within the system we employ a distribution function $f(\beta)$ which denotes for a uniaxial system the probability of finding the director at an angle β to a prescribed axis, in this work the shear axis. For those directors oriented along the shear direction the resultant SAXS patterns display uniaxially symmetric scattering, (Figure 2). This allows the orientation distribution function $f(\beta)$ which completely characterizes the orientational order to be written as the sum of orthogonal functions²¹

$$f(\beta) = \sum_{n=0}^{\infty} (4n+1) \bar{P}_{2n}(\cos \beta) P_{2n}(\cos \beta) \quad (1)$$

where the order parameters defined here, $\bar{P}_{2n}(\cos \beta)$, are ensemble averages of Legendre polynomials. These coefficients can be extracted directly from the SAXS patterns from the azimuthal distribution of the intensity at a fixed value of the magnitude of the scattering vector q , using a model for the scattering of a perfectly aligned system

$$\bar{P}_2 = \frac{\bar{P}_2^1}{\bar{P}_2^m} \quad (2)$$

where \bar{P}_2^1 is the normalized coefficient calculated from the observed X-ray scattering and \bar{P}_2^m is the coefficient calculated from the model. In this case the model for a

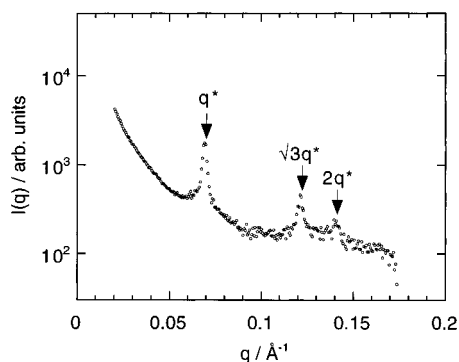


Figure 3. SAXS intensity profile obtained by integration in a vertical slice of the pattern in Figure 2a.

single unit (a director) is approximated to be an infinitely long rod, so that the orthogonal components of the scattering model are simplified to²²

$$\bar{P}_{2n}^m(\cos \beta) = \frac{(2n)!}{(-1)^n 2^{2n} (n!)^2} \quad (3)$$

and thus: $\bar{P}_2^m = -1/2$, $\bar{P}_4^m = 3/8$ and $\bar{P}_6^m = -5/16$. It should be noted that a complete description of the orientation function can be obtained from the scattering data between the azimuthal angles of $\phi = 0$ and $\phi = \pi/2$, and therefore the results presented in this paper, which were determined from a complete diffraction ring of $0 < \phi \leq 2\pi$, are averaged results from each of the four quadrants of the diffraction ring.

SAXS Experiments on Sheared Solutions

Representative SAXS data obtained during shear at 100 s^{-1} are presented in Figure 2. The pattern in the radial projection (Figure 2a) is highly anisotropic, with Bragg reflections along the meridian in the positional ratio $1:\sqrt{3}:2$ (see also Figure 3). This is consistent with a hexagonal structure in which the rods are oriented along the (horizontal) flow direction. The first-order Bragg reflection is superimposed on a ring of scattering from unoriented rods. This feature is characteristic of small-angle scattering patterns that have been observed for oriented samples of hexagonally packed rod phases in block copolymer melts^{9,12} and is ascribed to the presence of domains of rods that are misoriented with respect to the flow direction. Figure 2b shows a SAXS pattern in a tangential projection, which reveals that there is a uniaxial distribution of directors around the flow direction; i.e., the free rotation of domains occurs about this axis.

The SAXS pattern in Figure 2a was integrated in a vertical rectangular slice to provide the one-dimensional profile shown in Figure 3. From the location of the principal peak at $q^* = 0.069 \text{ Å}^{-1}$, the (10) spacing of hexagonally packed rods is determined to be $d = 91 \text{ Å}$. Assuming close-packing, the volume fraction of rods is $\Phi = 0.9$, and the micellar radius is calculated to be $r = 52 \text{ Å}$. Of course this provides an upper limit to the actual micellar radius. It is substantially smaller than the length of a fully extended $E_{18}B_{10}$ molecule

$$l_c \approx 1.21z \quad (4)$$

where z is the number of chain atoms (C and O) in the copolymer and 1.21 Å is the length per chain atom for

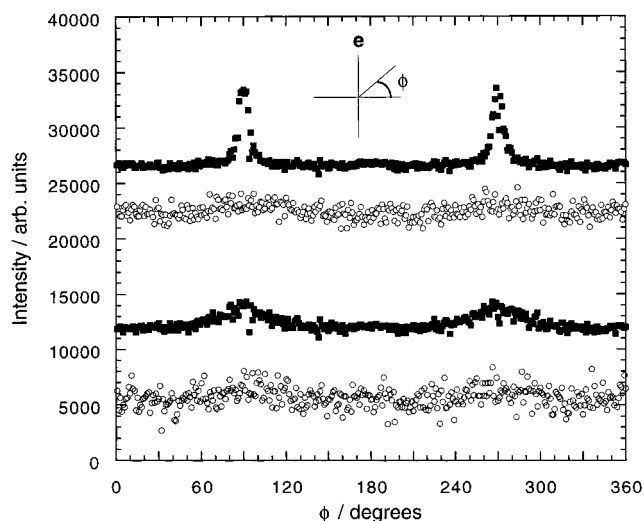


Figure 4. Scattered X-ray intensity as a function of azimuthal angle in the radial (■) and tangential (○) directions for the solution under shear at $\dot{\gamma} = 100 \text{ s}^{-1}$ (upper curves) and $\dot{\gamma} = 1 \text{ s}^{-1}$ (lower curves). The plots have been shifted along the ordinate for clarity.

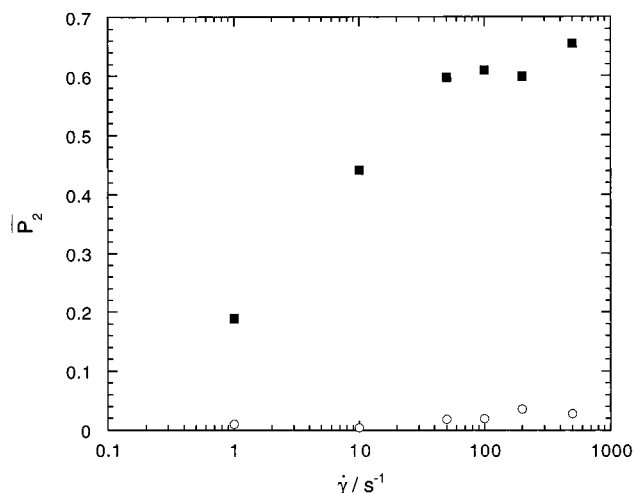


Figure 5. Global orientation parameter \bar{P}_2 in the radial (■) and tangential (○) directions as a function of shear rate.

the trans-planar chain.²³ This yields $l_c \approx 100 \text{ Å}$. With the present data, it is unfortunately impossible to determine the length of the rods.

Two typical pairs of azimuthal scattering profiles are shown in Figure 4; the higher statistical uncertainty in the data from the tangential aspect is due to the lower intensity of scattering from that projection, because of the greater thickness of cell wall which the X-ray beam must penetrate in this direction. Two principal features are indicated by Figure 4. First, increasing the shear rate significantly increases the anisotropy in the azimuthal distribution of the scattered intensity, as the directors align in the flow field. Second, it is evident that the orientation which was induced is observed only in the radial, and not the tangential, aspect. This latter observation is consistent with domains of rods rotating freely around the flow direction, producing a uniaxial distribution in the tangential projection.

A quantitative comparison of the second rank orientational order parameters extracted from the data in radial and tangential projections is made in Figure 5. It should be noted that at least 1000 cycles of shear were applied for each data point in this figure; i.e., the sample

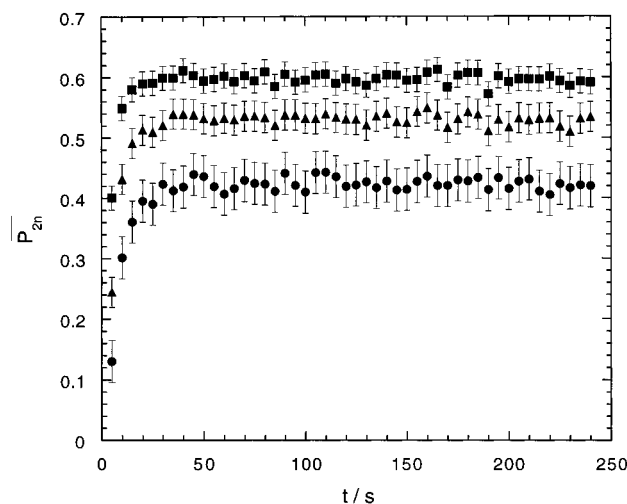


Figure 6. Development of the steady-state global orientation function coefficients \bar{P}_2 (■), \bar{P}_4 (▲), and \bar{P}_6 (●) as a function of time at a shear rate $\dot{\gamma} = 50 \text{ s}^{-1}$. The time $t = 0$ corresponds to the point at which shearing began.

was sheared at $\dot{\gamma} = 1 \text{ s}^{-1}$ for 20 min, although this was reduced for higher shear rates. The integration of this number of strain cycles was sufficient to ensure that a steady state orientation was reached. Figure 5 shows that the order parameter increases logarithmically with shear rate up to $\dot{\gamma} \sim 50 \text{ s}^{-1}$ in the radial aspect. Above $\dot{\gamma} \sim 50 \text{ s}^{-1}$, the orientation saturates to a level characterized by $\bar{P}_2 \sim 0.6$. Even in this regime the system was homogeneous, producing diffraction patterns such as those shown in Figure 2. In addition, the transmission factor monitored during the SAXS experiment did not vary dramatically with shear rate, indicating that any bubble formation due to foaming did not lead to substantial changes in the SAXS patterns. In the tangential aspect the order parameter remained close to zero for all shear rates investigated. The observation that the apparent saturation level of orientation within the $\text{E}_{18}\text{B}_{10}$ gel produces a value of \bar{P}_2 much less than unity is not surprising, as the presence of defects will prevent the director field from obtaining a perfect state of alignment. Additionally, even if a perfectly oriented director field was attained, the orientation parameter extracted from the SAXS pattern would still not realize unity due to the finite size and width of the scattering units (namely the domains of rods) and also the finite beam width and spectral breadth of the incident wavelength, for which these data were not corrected.

The time dependence for the establishment of an oriented texture within the gel immediately following the application of steady shear was also monitored in the radial aspect, and a typical profile is shown in Figure 6 for the case of a shear rate of $\dot{\gamma} \sim 50 \text{ s}^{-1}$. This reveals that saturation of orientation occurred within 20 s, i.e., after the accumulation of approximately 1000 shear units. The remaining data points clearly indicate that this orientation level reflected a stable, steady-state condition.

The relaxation of orientation was much slower, as illustrated by Figure 7. This shows the relaxation of the oriented state following the cessation of shear at $\dot{\gamma} \sim 100 \text{ s}^{-1}$, again using data from the radial aspect. The oriented structure relaxes to a steady orientation level over a time scale of about 1 h, with \bar{P}_4 relaxing more quickly than \bar{P}_2 . That there remains a residual (and

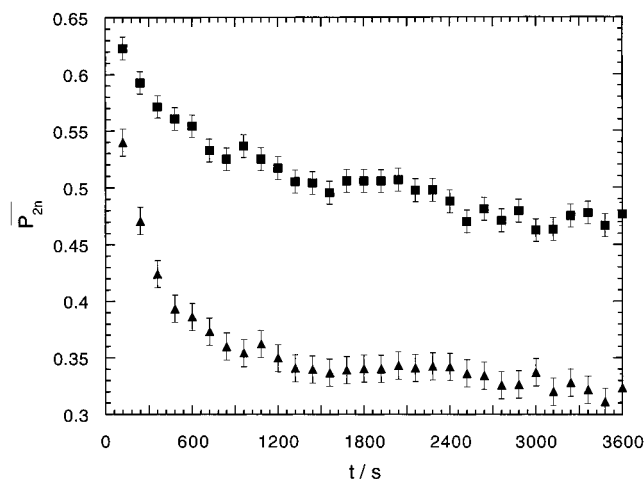


Figure 7. The relaxation of the global orientation function coefficients \bar{P}_2 (■) and \bar{P}_4 (▲) following shear at $\dot{\gamma} = 100 \text{ s}^{-1}$ for 10 min. The time $t = 0$ corresponds to the point at which shearing stopped.

significant) level of order after an hour of relaxation is not surprising, even though the domains of micelles might be anticipated to disorder somewhat as the defect texture relaxes around them. It is well known that shearing leads to permanently oriented structures in block copolymer melts and solutions. In a previous study of lyotropic solutions of polymeric cellulose derivatives it was also reported that, if sufficient deformation was applied to the polymer system, it retained a “memory” of the steady-state orientation, and did not recover the equilibrium texture which existed prior to the applied deformation.²⁴

Summary and Conclusions

The orientation of domains in the hexagonal phase of an $\text{E}_{18}\text{B}_{10}$ diblock copolymer gel was observed in SAXS patterns during the application of steady shear, with directors describing the orientation of the micellar domains aligning along the flow axis. The orientational order parameters induced by shear increased with shear rate. The second rank orientational order parameter increased linearly with a logarithmic increase in shear rate, up to a shear rate of $\dot{\gamma} \sim 50 \text{ s}^{-1}$, whereafter the orientation reached a plateau value at $\bar{P}_2 \sim 0.6$. Time-resolved measurements indicated that these steady-state orientation parameters were established after approximately 1000 cycles of shear, and upon cessation of shear, relaxed partially to an intermediate orientation over the time scale of $t \sim 1 \text{ h}$.

Acknowledgment. This work was supported by the EPSRC through Grants GR/K03982 and GR/K56117. The authors are grateful to Mark Nace of the Dow Chemical Company, Texas Operations, for the donation of the sample of $\text{E}_{18}\text{B}_{10}$. The data presented here were collected on beamline ID2 of the ESRF. The authors thank the station scientist, Olivier Diat, for his assistance.

References and Notes

- (1) Schick, M. J. *Nonionic surfactants*; Marcel Dekker: New York, 1967.
- (2) Hamley, I. W. “The Physics of Block Copolymers”, Oxford University Press, Oxford, U.K., in press.

- (3) Pople, J. A.; Hamley, I. W.; Fairclough, J. P. A.; Ryan, A. J.; Komanschek, B. U.; Gleeson, A. J.; Yu, G.-E.; Booth, C. *Macromolecules* **1997**, *30*, 5721.
- (4) Alexandridis, P.; Olsson, U.; Lindman, B. *Langmuir* **1997**, *13*, 23.
- (5) Balsara, N. P.; Dai, J. J. *J. Chem. Phys.* **1996**, *105*, 2942.
- (6) Marques, C. M.; Cates, M. E. *J. Phys. Fr.* **1990**, *51*, 1733.
- (7) Keller, A.; Pedemonte, E.; Willmouth, F. M. *Nature* **1970**, *225*, 538.
- (8) Hadziioannou, G.; Mathis, A.; Skoulios, A. *Colloid Polym. Sci.* **1979**, *257*, 7, 15, 136.
- (9) Almdal, K.; Bates, F. S.; Mortensen, K. J. *Chem. Phys.* **1992**, *96*, 9122.
- (10) Tepe, T.; Schulz, M. F.; Zhao, J.; Tirrell, M.; Bates, F. S.; Mortensen, K.; Almdal, K. *Macromolecules* **1995**, *28*, 3008.
- (11) Almdal, K.; Mortensen, K.; Koppi, K. A.; Tirrell, M.; Bates, F. S. *J. Phys. Fr. II* **1996**, *6*, 617.
- (12) Morrison, F. A.; Mays, J. W.; Muthukumar, M.; Nakatani, A. I.; Han, C. C. *Macromolecules* **1993**, *26*, 5271.
- (13) Winter, H. H.; Scott, D. B.; Gronski, W.; Okamoto, S.; Hashimoto, T. *Macromolecules* **1993**, *26*, 7236.
- (14) Richtering, W. *Prog. Colloid Polym. Sci.* **1997**, *104*, 90.
- (15) Lukaschek, M.; Grabowki, D. A.; Schmidt, C. *Langmuir* **1995**, *11*, 3590.
- (16) Nace, V. M.; Whitmarsh, R. H.; Edens, M. W. *J. Am. Oil Chem. Soc.* **1994**, *71*, 777.
- (17) Nace, V. M. *J. Am. Oil Chem. Soc.* **1996**, *73*, 1.
- (18) Yu, G.-E.; Yang, Y.-W.; Yang, Z.; Attwood, D.; Booth, C.; Nace, V. M. *Langmuir* **1996**, *12*, 3204.
- (19) Diat, O.; Roux, D.; Nallet, F. *J. Phys. II Fr.* **1993**, *3*, 1427.
- (20) Bösecke, P.; Diat, O.; Rasmussen, B. *Rev. Sci. Instrum.* **1995**, *66*, 1636.
- (21) Hamley, I. W.; Garnett, S.; Luckhurst, G. R.; Roskilly, S. J.; Pedersen, J. S.; Richardson, R. M.; Seddon, J. M. *J. Chem. Phys.* **1996**, *104*, 10046.
- (22) Lovell, R.; Mitchell, G. R.; *Acta Crystallogr.* **1981**, *A37*, 135.
- (23) Flory, P. J. *Statistical Mechanics of Chain Molecules*; Hanser: Munich, Germany, 1989; p 165.
- (24) Keates, P. A.; Mitchell, G. R.; Peuvrel-Disdier, E.; Navard, P. *Polymer* **1996**, *37*, 893.

MA9716490